Original Article

Establishing a carcinoembryonic antigen-associated competitive endogenous RNA network and forecasting an important regulatory axis in colon adenocarcinoma patients

Fangfang Liang[1,2]^, Yansong Xu[2], Haiping Zheng[1], Weizhong Tang[2]

[1]Department of Medical Oncology, Guangxi Medical University First Affiliated Hospital, Nanning, China; [2]College of Oncology, Guangxi Medical University, Nanning, China

Contributions: (I) Conception and design: F Liang; (II) Administrative support: W Tang; (III) Provision of study materials or patients: F Liang, Y Xu; (IV) Collection and assembly of data: F Liang; (V) Data analysis and interpretation: F Liang, H Zheng; (VI) Manuscript writing: All authors; (VII) Final approval of manuscript: All authors.

Correspondence to: Weizhong Tang, MD. College of Oncology, Guangxi Medical University, 22 Shuangyong Road, Nanning 530021, China. Email: tangweizhong0771@163.com; Haiping Zheng, MD. Department of Medical Oncology, Guangxi Medical University First Affiliated Hospital, 6 Shuangyong Road, Nanning 530021. China. Email: zhenghaiping@163.com.

Background: Colorectal cancer is one of the top five malignant tumors in the world in terms of morbidity and mortality. Numerous long non-coding RNAs (lncRNAs) are specifically expressed in tumours and can affect various types of human cancer by participating in competitive endogenous RNA (ceRNA) regulatory networks. However, the specific mechanisms and complex networks of ceRNA regulatory patterns in colon adenocarcinoma (COAD) remain unclear.

Methods: Using The Cancer Genome Atlas (TCGA) database, we identified the differentially expressed lncRNA, microRNA (miRNA), and messenger RNA (mRNA) between colon cancer and normal tissues, as well as between groups with high and low CEACAM5 expression. Then, we constructed CEACAM5-related ceRNA networks, established the key lncRNA-miRNA-mRNA regulatory axis, and explored the biological mechanisms of this axis and its clinical significance in colon cancer from multiomic aspects.

Results: We constructed a ceRNA network of 18 lncRNAs, 177 miRNAs, and 25 mRNAs associated with CEACAM5 and finally established the key *LCMT1-AS2*/miR-454-3p/ribosomal protein S6 kinase A5 (RPS6KA5) axis associated with overall survival. Subsequent investigations have indicated that this regulatory axis could potentially participate in the progression of COAD and exert influence on the therapeutic outcomes of chemotherapy and immunotherapy. It may be involved in the PI3K-Akt signaling pathway and may modify the tumor immune microenvironment and influence the course of COAD. Additionally, it may be related to ferroptosis, N6-methyladenosine (m6A) methylation, and tumor stemness and interfere with the sensitivity of tumor cells to 5-fluorouracil and immunotherapy.

Conclusions: The LCMT1-AS2/RPS6KA5 axis may be instrumental in tumor progression, potentially acting as a prognostic biomarker and therapeutic target.

Keywords: Colon adenocarcinoma (COAD); CEACAM5; competitive endogenous RNA (ceRNA); ribosomal protein S6 kinase A5 (*RPS6KA5*)

Submitted Jan 15, 2024. Accepted for publication Feb 19, 2024. Published online Feb 28 2024.
doi: 10.21037/jgo-24-43
View this article at: https://dx.doi.org/10.21037/jgo-24-43

^ ORCID: 0000-0001-9337-4375.

Introduction

According to the Global Cancer Statistics 2020, the morbidity of colorectal cancer (CRC) ranks as the third highest worldwide, while its mortality rate is the second leading cause of oncological fatalities globally (1). CEACAM5 encodes a cell surface glycoprotein, which represents the founding member of the carcinoembryonic antigen (CEA) protein family. CEA is synthesized in the cytoplasm and then secreted through the cell membrane into the extracellular space, entering the surrounding body fluids. CEA levels in normal adult colonic tissues and sera are usually low, but inflammatory responses and multiple solid tumors can lead to elevated serum CEA level (2,3). Serum CEA has been utilized as a broad-spectrum tumor marker and therapeutic target for various solid tumors, including CRC (4,5). Furthermore, CEACAM5 plays a role in promoting the development of colon cancer as a homophilic or specific adhesion molecule (6) and indirectly influences colon cancer development through unique characteristics recognized by the immune system (7). Mutated CEACAM5 can promote CRC carcinogenesis by modifying the gut microbiota (8).

Long non-coding RNAs (lncRNAs) have no or limited protein-coding capacity. Numerous lncRNAs are dysregulated in various types of cancer and are associated with cell proliferation, migration, apoptosis, angiogenesis, drug resistance, and poor prognosis (9). However, the functions of most lncRNAs remain unclear. The competitive endogenous RNA (ceRNA) hypothesis, which reveals a new pattern of gene expression regulation (10), provides a pathway for predicting the noncoding function of any uncharacterized RNA transcript (11). Certain lncRNAs can function as ceRNAs, harboring the same microRNA (miRNA) response elements as messenger RNAs (mRNAs). Consequently, they establish a competitive interaction for the same type of miRNAs. In this manner, lncRNAs indirectly modulate the expression levels of mRNAs, thereby orchestrating cellular functions (12). For instance, the pseudogene *PTENP1* functions as a miRNA sponge to modulate the expression of *PTEN*, which plays a role in many cancer pathways (13).

Elucidating the molecular mechanisms of the development and progression of colon cancer and identifying promising biomarkers are critical to the identification of novel therapeutic targets and improvement of patient outcomes (14). Considering the critical role of CEACAM5, we endeavor to construct a CEACAM5-associated ceRNA network utilizing bioinformatics techniques, with the objective of identifying potential promising biomarkers or therapeutic targets. First, the clinical and gene-expression data of colon adenocarcinoma (COAD) in The Cancer Genome Atlas (TCGA) were used in identifying differential genes for colon cancer and normal tissue s and for CEACAM5 high- and low-expression groups. Then, a database software was used in predicting lncRNA-miRNA and miRNA-mRNA binding pairs, and lncRNA-miRNA-mRNA triple regulatory networks were constructed. Prognostic and correlation analyses were then performed on clinical pathological factors in the ceRNA regulatory networks, and the key *LCMT1-AS2*/ribosomal protein S6 kinase A5 (RPS6KA5) regulatory axis was determined. Finally, the biological mechanism of the *LCMT1-AS2*/*RPS6KA5* axis and its possible clinical significance in colon cancer were explored from a multiomic perspective (*Figure 1*). We present this article in accordance with the TRIPOD reporting checklist (available at https://jgo.amegroups.com/article/view/10.21037/jgo-24-43/rc).

Highlight box

Key findings

- The *LCMT1-AS2*/ribosomal protein S6 kinase A5 (*RPS6KA5*) axis may play an important role in tumor progression and is an important prognostic factor for predicting the clinical outcome of colon adenocarcinoma (COAD).

What is known and what is new?

- Growing evidence underscores the role of competitive endogenous RNA (ceRNA) networks in COAD. The CEACAM5-encoded protein, a COAD biomarker, also has significant influence via other pathways.
- A CEACAM5-associated lncRNA-miRNA-mRNA network was constructed, ultimately identifying the pivotal LCMT1-AS2/miR-454-3p/RPS6KA5 axis associated with overall survival. This axis may be instrumental in tumor progression, potentially acting as a prognostic biomarker and therapeutic target.

What is the implication, and what should change now?

- The innovation of this study is to CEACAM5-associated ceRNA networks and establish the key regulatory axis based on the ceRNA hypothesis, and this research method is relatively rare at present. In addition, the bioinformatics analysis methods we employed are relatively rich and complex, and the research idea and design are unique and innovative.

Methods

Data preparation and management

We downloaded the sequencing data of patients with COAD and clinical data from TCGA (https://portal.gdc.

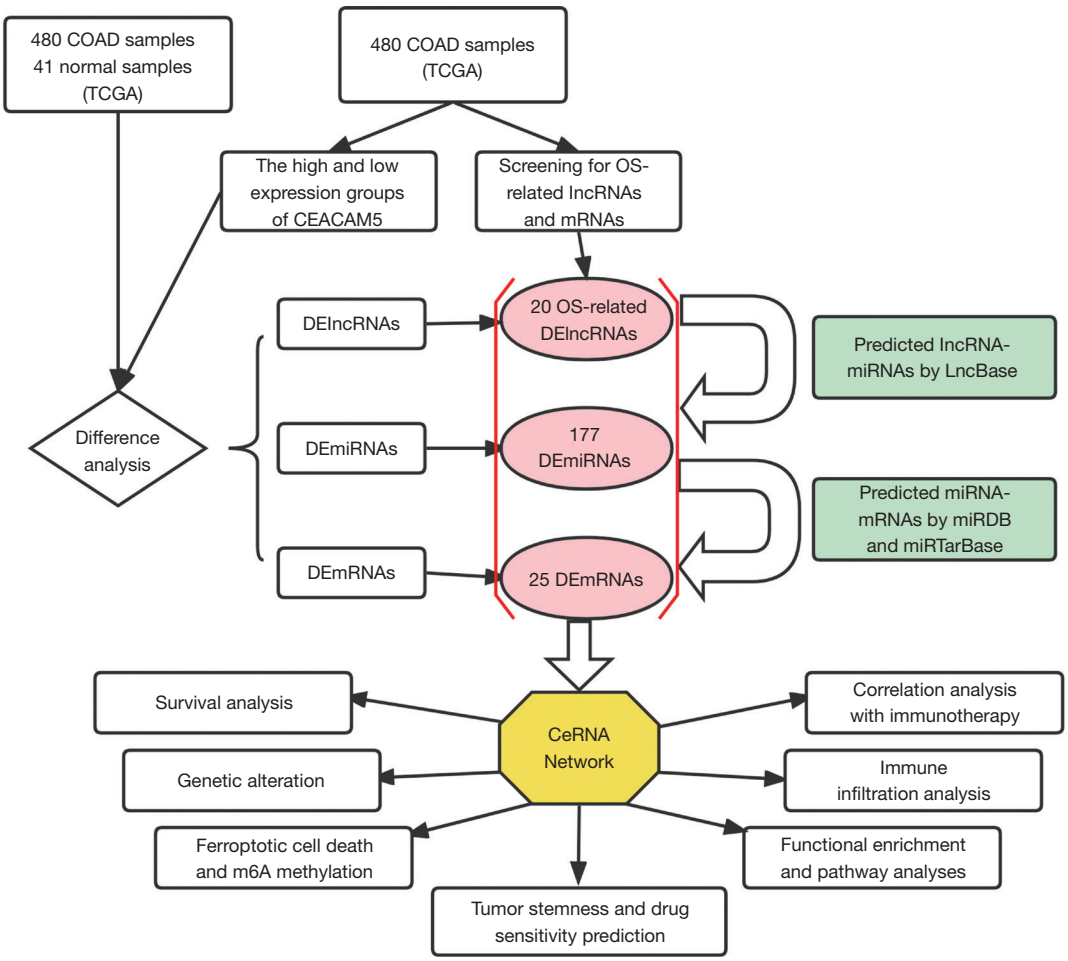

Figure 1 Flowchart of ceRNA construction and analysis. COAD, colorectal adenocarcinoma; TCGA, The Cancer Genome Atlas; OS, overall survival; lncRNAs, long non-coding RNAs; mRNA, messenger RNA; DE, differentially expressed; miRNA, microRNA; ceRNA, competitive endogenous RNA; m^6A, N6-methyladenosine.

cancer.gov/) database. We obtained data from the University of California Santa Cruz (UCSC) Xena browser (http://xena.ucsc.edu) and compared them with healthy tissues. The somatic mutations of TCGA-COAD were downloaded and visualized using the maftools R package (15). The gene expression profiles of GSE10950 were extracted from the Gene Expression Omnibus (GEO; https://www.ncbi.nlm.nih.gov/geo/) for the verification of the analysis results. The Cancer Cell Line Encyclopedia (CCLE; https://portals.broadinstitute.org/ccle) and the Human Protein Atlas (HPA; http://www.proteinatlas.org/) databases were used in verifying gene expression in tumor cell lines at the protein level. The genomic features were studied using the cBioPortal database (http://www.cbioportal.org/). The study was conducted in accordance with the Declaration of Helsinki (as revised in 2013).

Identification of differential genes

Differentially expressed genes (DEGs) were identified using the DESeq2 (version 1.26.0) R package (16). Volcano plots and heatmaps were plotted using ggplot2 (version 3.3.3) and ComplexHeatmap R (version 2.2.0) packages, respectively. All survival analyses were conducted using the Cox proportional hazard model with R survival package (version 3.2.10).

Establishment of CEACAM5-associated ceRNA networks

According to the ceRNA hypothesis, lncRNAs in the

cytoplasm can serve as natural sponges to adsorb miRNAs, thereby indirectly regulating mRNA abundance and affecting protein levels (12). First, we predicted the target-gene miRNAs (threshold =0.7) of lncRNAs by using LncBase Predicted v.2 (http://www.microrna.gr/LncBase/) and then predicted the intersection of the resulting miRNAs with differentially expressed miRNAs (DEmiRNAs). Second, the target gene mRNAs of miRNAs were predicted using miRWalk V3 version (17), which was required to satisfy miRDB (18,19) and miRTarBase (20). Similarly, the predictions were intersected with differentially expressed mRNAs (DEmRNAs) and overall survival (OS)-related mRNAs. Finally, the resulting miRNA-mRNA and lncRNA-miRNA pairs were integrated for ceRNA network construction, and the networks were plotted using Cytoscape software (https://cytoscape.org/).

Functional mechanism study

Taking the median expression of *RPS6KA5* as the cutoff, we divided TCGA-COAD patients into high- and low-expression groups. Gene Ontology (GO) and Kyoto Encyclopedia of Genes and Genomes (KEGG) pathway enrichment analysis [threshold: P<0.05 or false discovery rate (FDR) <0.05] was performed using the R clusterProfiler package (version 3.18.0) (21). Further functional mechanism studies were performed. Ferroptosis and ferroptosis-related genes (FRGs) can exert oncogene and tumor suppressor effects on various cancer types (22), and most FRGs are abnormally expressed in multiple cancer types (23). In our study, 24 FRG expression differences were compared between COAD tissues and normal colon tissues, and between subgroups with different expression levels of *RPS6KA5* in COAD patients. Furthermore, we evaluated the expression of m^6A writers, erasers, and readers in the subgroup with the lowest *RPS6KA5* expression levels and the subgroup with the highest expression levels. Malta *et al.* calculated DNA methylation-based stemness index (mDNAsi) and mRNA expression-based stemness index (mRNAsi) by using a logistic regression machine learning algorithm to reflect the tumor stemness, and the two stemness indexes exhibited excellent consistency in most tumors (24). We calculated mRNAsi and compared the tumor stemness of the two groups. The Genomics of Drug Sensitivity in Cancer database (GDSC; https://www.cancerrxgene.org/) was used for susceptibility analysis. We then calculated the half-maximal inhibitory concentration (IC50) values of 5-fluorouracil (5-FU) for each sample (all parameters were kept as default) through ridge regression by using the pRRophetic R package (25) and compared the two groups.

Immune infiltration and immune scores

The ESTIMATE R package (version 1.0.13) (26) was used in estimating the Immune, Stromal and ESTIMATE scores of the tumor microenvironment for each tumor sample, and then their correlation with gene expression levels was analyzed using Pearson correlation. Using the Tumor IMmune Estimation Resource (TIMER; http://timer.cistrome.org/) database, we analyzed the relationships between levels of immune cells infiltration and gene copy numbers in the 'SCNA' module between several immune cells and gene expression in the 'Gene' module and between immune cells infiltration level and COAD prognosis.

Statistics analysis

All survival analyses were performed using log-rank test and Cox regression analysis with R survival package (version 3.2.10). Wilcoxon rank sum test was used in comparing two groups, and Kruskal-Wallis test was performed in comparing more than two groups. All statistical analyses were conducted in R (R version 3.6.3). All hypothesis tests were bilateral, and the difference was considered to be statistically significant when P<0.05.

Results

Expression and prognostic value of CEACAM5 in colon cancer

CEACAM5 expression level was significantly increased in CRC and significantly higher in other solid tumors, such as lung adenocarcinoma, lung squamous-cell carcinoma, pancreatic cancer, and gastric cancer, than that in normal tissues (*Figure 2A*). Immunohistochemical images obtained from the HPA database also confirmed elevated CEACAM5 expression in colon cancer tissue (*Figure 2B*). To determine whether the gene was associated with prognosis, Cox regression was used in analyzing the correlation between genes and OS, disease-specific survival (DSS), and progression-free interval (PFI). The results suggested that the CEACAM5 high-expression group had better OS, DSS, and PFI (*Figure 2C*) than the low-expression group, contrary to the prognostic predictive effect of serum CEACAM5 on

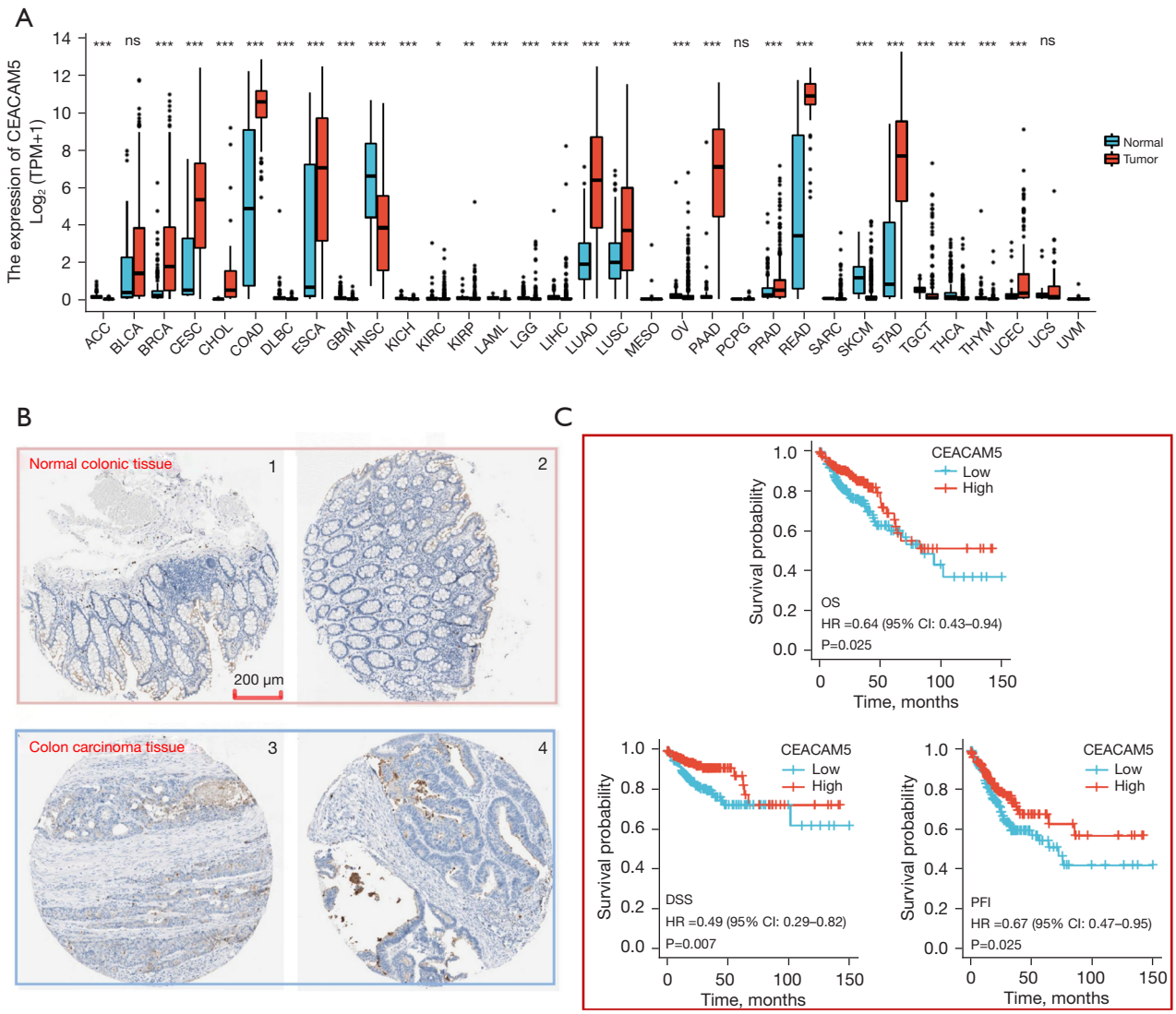

Figure 2 The expression of CEACAM5 in cancer tissues and its relationship with prognosis of COAD patients. (A) Pan-cancer analysis showed that CEACAM5 was significantly highly expressed in various cancerous tissues, such as COAD. (B) Immunohistochemical images in the HPA database show: CEACAM5 is highly expressed in COAD tissues (1 and 2 are normal colon tissues, https://www.proteinatlas.org/ENSG00000105388-CEACAM5/tissue/colon; 3 and 4 are COAD tissues, https://www.proteinatlas.org/ENSG00000105388-CEACAM5/pathology/colorectal+cancer.) (C) The CEACAM5 low-expression group had poorer OS, DSS, and PFI. *, P<0.05; **, P<0.01; ***, P<0.001. TPM, transcripts per million; ns, not significant; OS, overall survival; HR, hazard ratio; COAD, colorectal adenocarcinoma; HPA, Human Protein Atlas; DSS, disease-specific survival; PFI, progression-free interval.

colon cancer (27,28).

To understand the mechanisms underlying the abnormally high expression of CEACAM5 in colon cancer tissues, we analyzed the genetic mutations and copy numbers of CEACAM5 in the TCGA-COAD dataset (594 patients) on cBioPortal (Figure S1). The copy number value of CEACAM5 was positively correlated with mRNA expression (Spearman r=0.18; P<0.05). Increased gene copy number may be one of the main mechanisms causing the upregulation of CEACAM5 in CRC.

Identification of DEGs

Given the important role of CEACAM5 in colon cancer,

the next steps were to construct a lncRNA-miRNA-mRNA triple regulatory network and to explore its possible clinical value. DEGs were identified in the high- and low-expression groups of CEACAM5 and between the COAD and para-tumor tissue samples from the datasets in TCGA. The threshold for lncRNA was set at $|\log_2$[fold change (FC)]$|$ >1.5 and adjusted P value (P.adj) <0.05; miRNA threshold was set at $|\log_2(FC)|$ >1 and P.adj <0.05; miRNA threshold was set at $|\log_2(FC)|$ >0.7 and P.adj <0.05.

Samples with high CEACAM5 expression were compared with samples with low CEACAM5 expression. We identified 1,845 differentially expressed lncRNAs (DElncRNAs; 1 upregulated and 1,844 downregulated), 225 DEmiRNAs (0 upregulated and 225 downregulated), and 2,531 DEmRNAs (108 upregulated and 2,423 downregulated; Figure S2A-S2C). Paired differential analysis comparing COAD and matching normal colon tissues identified 2,774 DElncRNAs (2,289 upregulated and 485 downregulated), 148 DEmiRNAs (132 upregulated and 16 downregulated), and 7,561 DEmRNAs (3,980 upregulated and 3,581 downregulated; Figure S2D-S2F).

Construction of CEACAM5-associated ceRNA network

Univariate analysis of clinical and RNA-sequencing (RNAseq) data from the TCGA-COAD cohort (29) was performed using a Cox proportional risk regression model. With P<0.05 as the threshold, 464 lncRNAs and 1,479 mRNAs were identified as related to OS. Subsequently, 464 lncRNAs were intersected with the 1,845 DElncRNAs and 2,774 DElncRNAs determined from the previous analysis for production of 20 lncRNAs, which were entered into the LncBase database. MiRNAs bound to them were predicted (threshold =0.7). The resulting 212 miRNAs were intersected with 225 DEmiRNAs for the production of 177 miRNAs. Then, miRWalk was used in predicting miRNA target genes. The prediction results of miRDB and miRTarBase were used simultaneously, and 1,140 mRNAs were obtained. These mRNAs were then intersected with 7,561 DEmRNAs and 1,479 OS-associated mRNAs for the production of 25 mRNAs. Afterwards, the ceRNA networks of 18 lncRNAs, 177 miRNAs, and 25 mRNAs were visualized using Cytoscape (Figure S3).

The lncRNA *LCMT1-AS2* might bind to abundant miRNAs as a ceRNA, and thus we constructed *LCMT1-AS2*-162miRNA-20mRNA networks (*Figure 3A*). Correlation analyses between *LCMT1-AS2* and each mRNA revealed that *LCMT1-AS2* was significantly associated with *RPS6KA5*, *ABCB5*, *PRRT2*, and *BAHD1* (Pearson r>0.4, *Figure 3B*).

We obtained four *LCMT1-AS2* regulator axes, namely, miR-4306/*PRRT2*, miR-4446-5p or miR-454-3p/*RPS6KA5*, miR-4676-5p/*ABCB5* and miR-506-3p/*BAHD1*. Given that the cell localization of lncRNAs determined the underlying mechanisms, the subcellular localization of *LCMT1-AS2* was analyzed using LNCipedia (https://lncipedia.org/) and lncLocator (http://www.csbio.sjtu.edu.cn/bioinf/lncLocator/). *LCMT1-AS2* had five transcripts primarily located in the cytoplasm and cytosol (*Table 1*).

Clinical significance of the LCMT1-AS2 regulatory axis in COAD

To clarify the clinical significance of the ten genes obtained from the above analysis in COAD, we adopted multi-omics methods to explore them in subsequent studies. First, we evaluated the expression of the genes in the tumor tissues of patients with COAD. MiR-4676-5p was significantly downregulated in the COAD tissues compared with adjacent tissues, whereas miR-4446-5p expression did not change significantly. MiR-454-3p, miR-506-3p, and miR-4306 exhibited extremely low levels of expression in eight adjacent non-cancerous tissues, but were present in higher levels in colon cancer tissues. *LCMT1-AS2*, *RPS6KA5*, *PRRT2*, *ABCB5*, and *BAHD1* were significantly underexpressed in the COAD tissues in contrast to their expression in normal colon tissues (*Figure 4A*).

Cox regression analysis then revealed that patients with COAD in the high *LCMT1-AS2*, *ABCB5*, *PRRT2*, or *BAHD1* group had poorer OS than those in the low-expression groups, whereas the *RPS6KA5* low-expression group had poorer OS and miR-454-3p and miR-4676-5p expression levels were independent of OS (*Figure 4B*). Owing to the extremely low expression of more than half of the specimens, the correlations of miR-506-3p, miR-4306, and miR-4446-5p with OS was not analyzed.

Correlation analysis between gene expression levels and clinicopathological parameters was subsequently performed. Wilcoxon rank-sum test analysis showed that miR-454-3p expression was significantly associated with lymphatic invasion and perineural invasion and independent of gender, T stage, N stage, distant metastasis, pathological stage, and serum CEA expression level. MiR-4676-5p was associated with distant metastasis and lymphatic invasion and was not associated with other clinical factors. *RPS6KA5* expression was related to tumor-node-metastasis (TNM)

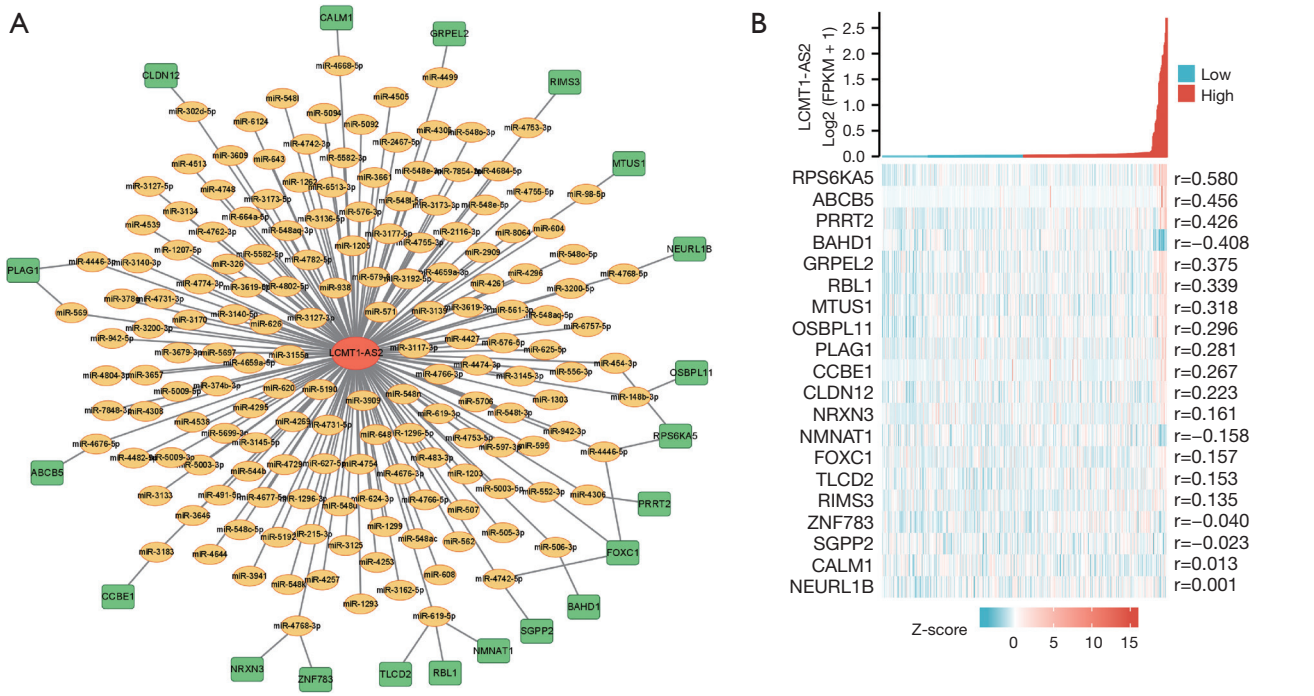

Figure 3 Visualization of the LCMT1-AS2-mediated ceRNA networks and analysis of the correlation between LCMT1-AS2 and the 20 mRNAs within the ceRNA networks. (A) *LCMT1-AS2*-162miRNA-20mRNA regulatory networks. (B) Correlation analysis of *LCMT1-AS2* with 20 mRNAs. FPKM, fragments per kilobase of exon per million fragments mapped; ceRNA, competitive endogenous RNA; miRNA, microRNA; mRNA, messenger RNA.

Table 1 Cell localization of five transcripts of LCMT1-AS2

Subcellular locations (score)	LCMT1-AS2:1	LCMT1-AS2:2	LCMT1-AS2:3	LCMT1-AS2:4	LCMT1-AS2:5
Cytoplasm	0.234449659	0.265325317	0.762889736	0.492690767	0.234449659
Nucleus	0.087777402	0.098903241	0.176458993	0.383300021	0.087777402
Ribosome	0.238028817	0.241641621	0.010304191	0.02009132	0.238028817
Cytosol	0.417439425	0.370390729	0.044421524	0.080425189	0.417439425
Exosome	0.022304697	0.023739093	0.005925556	0.023492704	0.022304697

stage, pathological stage, and lymphatic invasion. *PRRT2* expression was significantly associated with N staging and pathological grading (Figure S4). *LCMT1-AS2*, *ABCB5*, or *BAHD1* expression level was not correlated with clinical pathological factors.

A significant positive correlation between *LCMT1-AS2* and *RPS6KA5* was found (*Figure 3B*; Spearman r=0.58, P<0.05), and both were correlated with the OS of patients with COAD. Alternatively, we detected significantly high expression of miR-454-3p and low expression of *RPS6KA5* in COAD tissues, and both were related to clinicopathological factors. Therefore, the *LCMT1-AS2/miR-454-3p/RPS6KA5* axis was finally established. To understand the mechanism of action of this regulatory axis in colon cancer, we performed a detailed analysis of *RPS6KA5*.

Expression validation of RPS6KA5 and enrichment analysis

Independent cohort data (GSE10950: 24 pairs of COAD samples and paracancerous samples) presented within

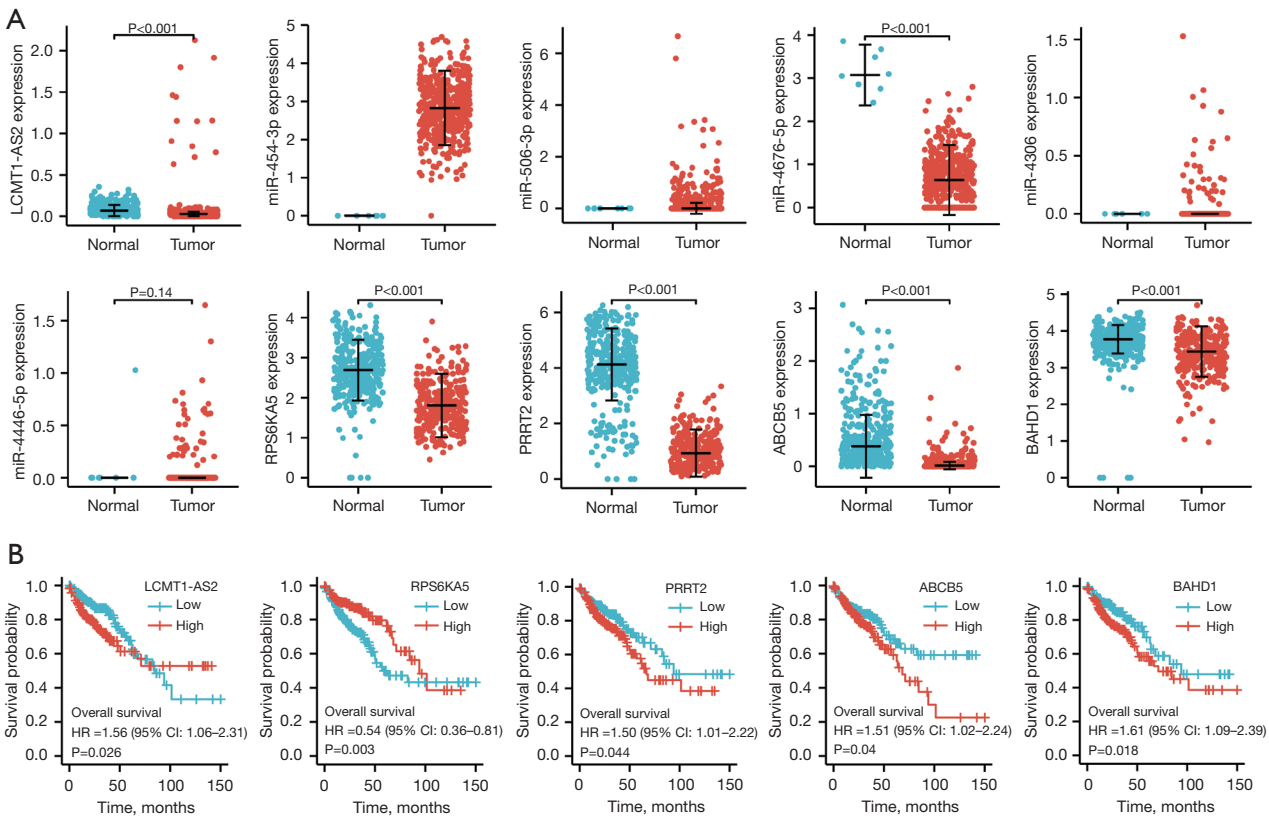

Figure 4 Expression level and prognostic value of ten hub genes. (A) Differential expression of ten genes in COAD and normal colonic tissues in the *LCMT1-AS2* regulatory axis. (B) Kaplan-Meier survival curve. COAD, colorectal adenocarcinoma; HR, hazard ratio.

GEO database provided evidence of the downregulation of *RPS6KA5* expression in cancer tissues (*Figure 5A*). Similarly, the representative images of immunohistochemical staining from the HPA database suggested that *RPS6KA5* had low expression level in the colon cancer tissues (*Figure 5B*). Moreover, the expression levels of *RPS6KA5* in various malignant tumor cell lines (Figure S5) and CRC cell lines were queried in CCLE database (Figure S6).

Figure 5C shows the somatic mutation landscape in TCGA-COAD cohort, with a mutation rate of about 2% in *RPS6KA5* and a higher frequency of somatic mutations in the *RPS6KA5* high-expression group. The mutation types, structural variation, and copy number alterations (CNAs) of *RPS6KA5* for 594 CRC patient samples from TCGA database were queried in the cBioPortal database (*Figure 5D,5E*). A significant positive association was found between the copy number value of *RPS6KA5* and mRNA expression (Spearman r=0.37; P<0.05).

Differential expression analysis was performed on the *RPS6KA5* high-expression and low-expression groups [|log(FC)| >1.5; *Figure 6A,6B*]. Subsequently, 170 upregulated genes and 29 downregulated genes were subjected to enrichment analysis (*Figure 6C*). The two gene sets were mostly enriched in the PI3K-Akt signaling pathway.

Analysis of functional mechanism related to RPS6KA5

Patients with COAD were evenly divided into four groups according to their *RPS6KA5* expression levels (*Figure 7A*). The top 25% group (*RPS6KA5*$^{high25\%}$) had the longest median OS (7.1 years), and the bottom 25% group (*RPS6KA5*$^{low25\%}$) had the shortest median OS (5 years; *Figure 7B*). The areas under the receiver operating characteristic (ROC) curve (AUCs) for predicting 1-, 3- and 5-year survival probability were 0.542, 0.584, and 0.644, respectively (*Figure 7C*).

Ferroptosis

Ferroptosis is an iron-mediated regulatory cell death and

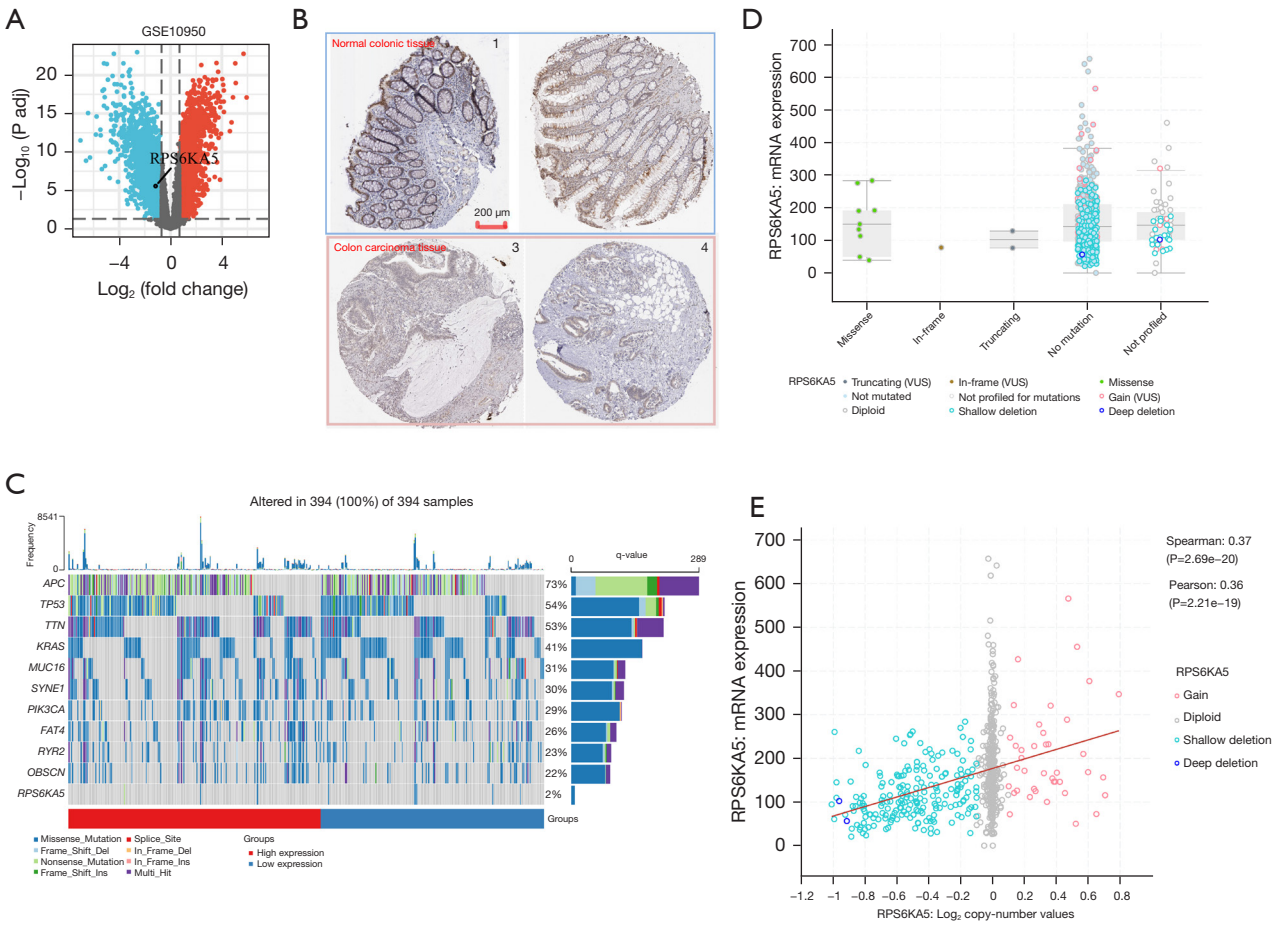

Figure 5 The aberrant expression and genetic alteration of *RPS6KA5* in COAD. (A) GEO: the GSE10950 cohort verified that *RPS6KA5* expression was downregulated in colon cancer tissues (red represents upregulated genes, blue represents downregulated genes, and grey represents non-significant genes). (B) Immunohistochemical staining images in the HPA database suggested that *RPS6KA5* was underexpressed in COAD tissues (1 and 2 are normal colon tissues, https://www.proteinatlas.org/ENSG00000100784-RPS6KA5/tissue/colon#img; 3 and 4 are COAD tissues, https://www.proteinatlas.org/ENSG00000100784-RPS6KA5/pathology/colorectal+cancer#img). (C) Oncoplot shows the somatic landscape of TCGA-COAD cohort. Genes are arranged according to their mutation frequency, while samples are sorted by disease histology, as denoted in the annotation bar (at the bottom). Side bar graph displays the –log10-transformed q-values, as estimated using MutSigCV. Waterfall plot displays the mutation information of each gene in each sample, where various mutation types are represented by different colors at the bottom with specific annotations. The barplot above the legend displays the number of mutation burdens. (D) Relationship between *RPS6KA5* genomic alterations and mRNA expression in the TCGA-COAD cohort of the cBioPortal database. (E) *RPS6KA5* copy number was positively correlated with mRNA expression. P.adj, adjusted P value; *RPS6KA5*, ribosomal protein S6 kinase A5; VUS, variant of uncertain significance; mRNA, messenger RNA; COAD, colorectal adenocarcinoma; GEO, Gene Expression Omnibus; HPA, Human Protein Atlas; TCGA, The Cancer Genome Atlas; MutSigCV, Mutation Significance in Cancer Version.

has the dual role of promoting and inhibiting tumors during tumorigenesis. It affects the efficacy of chemotherapy, radiotherapy, and immunotherapy (30). We compared the expression levels of 24 FRGs in the *RPS6KA5*$^{high25\%}$ and *RPS6KA5*$^{low25\%}$ groups to determine whether *RPS6KA5* is associated with ferroptosis. Wilcoxon test suggested that the expression of 16 FRGs differed significantly between the two groups (*Figure 8A*), indicating that *RPS6KA5* is involved in regulating ferroptosis in colon cancer.

M6A methylation

M^{6}A methylation is one of the most common epigenetic modifications in mRNA. Enzymes involved in m^{6}A modification can cause various diseases, including

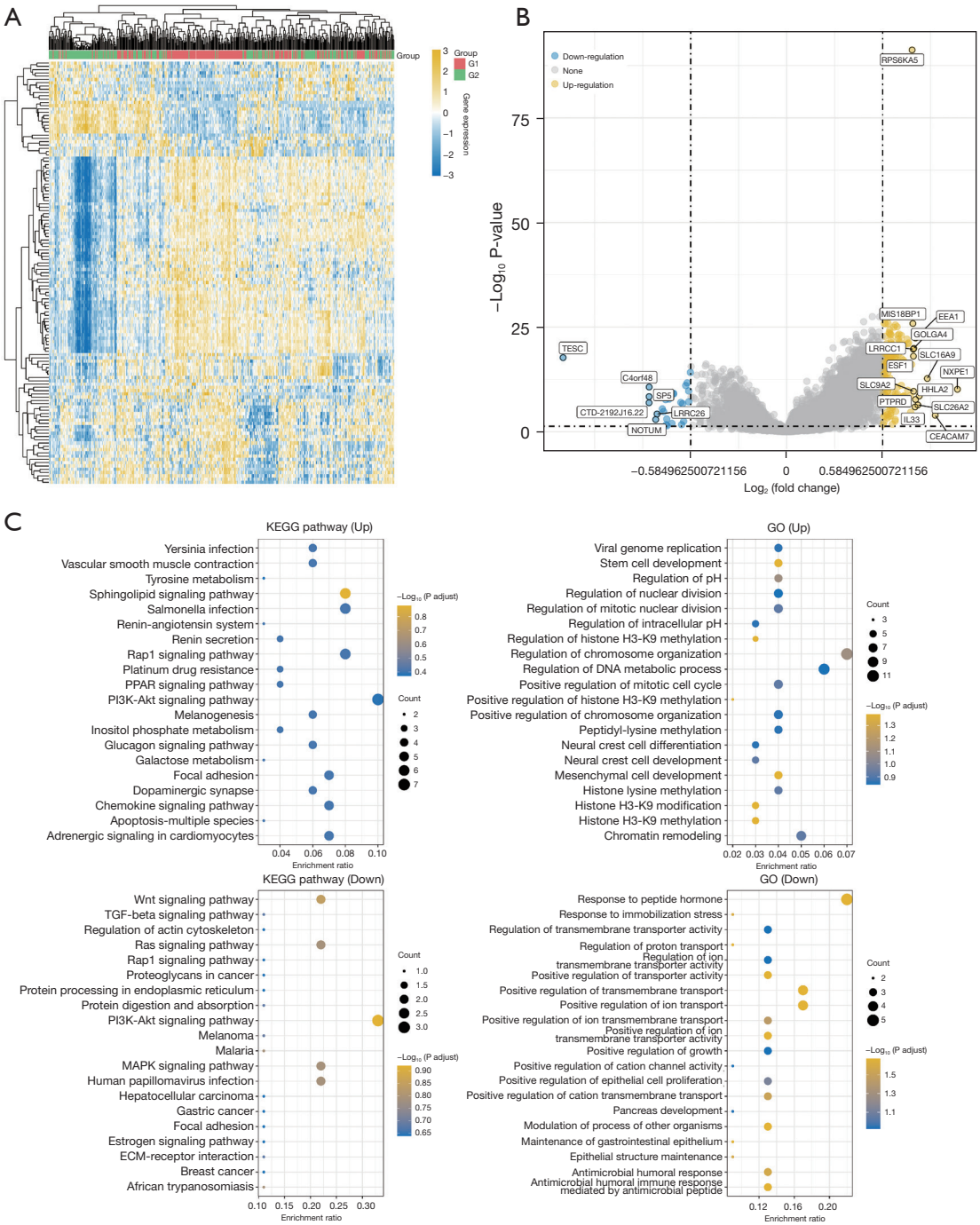

Figure 6 Differential expression analysis and enrichment analysis. (A,B) Differential gene heat map (A) and volcano map (B) of *RPS6KA5* high- and low-expression groups. (C) KEGG and GO enrichment analysis of differentially up-regulated (top two figures)/down-regulated (bottom two figures) genes between *RPS6KA5* high/low group. In the enrichment result, P<0.05 or FDR <0.05 is considered to be a meaningful pathway. G1, high expression group of *RPS6KA5*; G2, low expression group of *RPS6KA5*; *RPS6KA5*, ribosomal protein S6 kinase A5; KEGG, Kyoto Encyclopedia of Genes and Genomes; GO, Gene Ontology; FDR, false discovery rate.

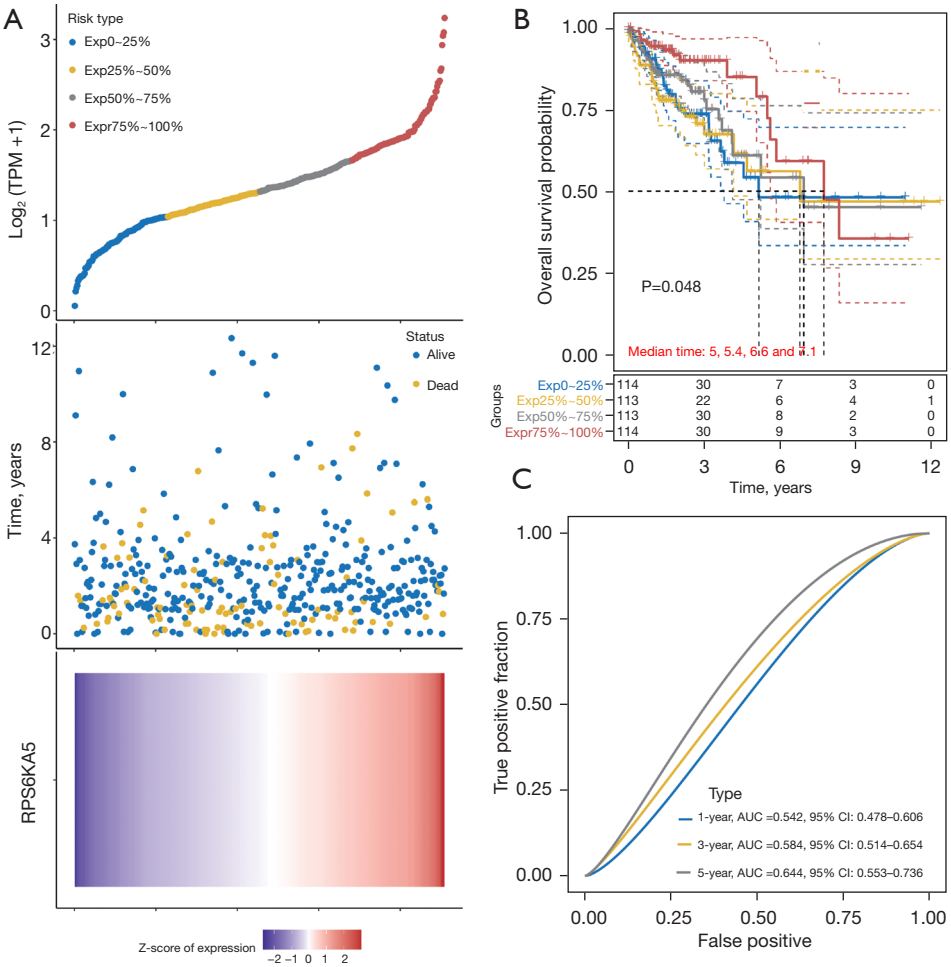

Figure 7 Association between expression of *RPS6KA5* and prognosis in COAD. (A) From top to bottom: gene expression curves, survival status plots, and gene expression heat maps for different groups. (B) Survival curves of different subgroups. (C) *RPS6KA5* time-dependent ROC plots predicting 1-, 3-, and 5-year total survival. *RPS6KA5*, ribosomal protein S6 kinase A5; AUC, area under the curve; CI, confidence interval; COAD, colon adenocarcinoma; ROC, receiver operating characteristic.

tumors (31). Herein, we found that compared with the *RPS6KA5*$^{low25\%}$ group, the *RPS6KA5*$^{high25\%}$ group had 16 genes correlated with the three types of regulatory enzymes (m^6A writers, readers, and erasers) with high expression levels. Only *RBM15B*, *YTHDF1*, *IGF2BP1*, and *IGF2BP2* were not expressed differently between the two groups (*Figure 8B*).

Tumor stemness

Cancer progression is accompanied by the gradual loss of tumor cell differentiation phenotype and the acquisition of stem cell-like characteristics (24), and the stemness of cancer cells is closely related to tumor proliferation and metastasis and drug resistance (31). Based on the one-class logistic regression (OCLR) algorithm (24), the degree of stemness of cancer samples can be assessed by calculating their stemness index. We found that the mRNAsi of COAD tissues was markedly increased compared with that of normal colon tissues, and the mRNAsi of the *RPS6KA5*$^{high25\%}$ group was significantly higher than that of the *RPS6KA5*$^{low25\%}$ group (*Figure 8C*).

Chemotherapy

5-FU is one of the most commonly used chemotherapy drugs for colon cancer. Using the GDSC database, we determined whether *RPS6KA5* expression levels affected the response of patients with colon cancer to drug therapy with 5-FU. The IC50 of 5-FU in each sample was calculated,

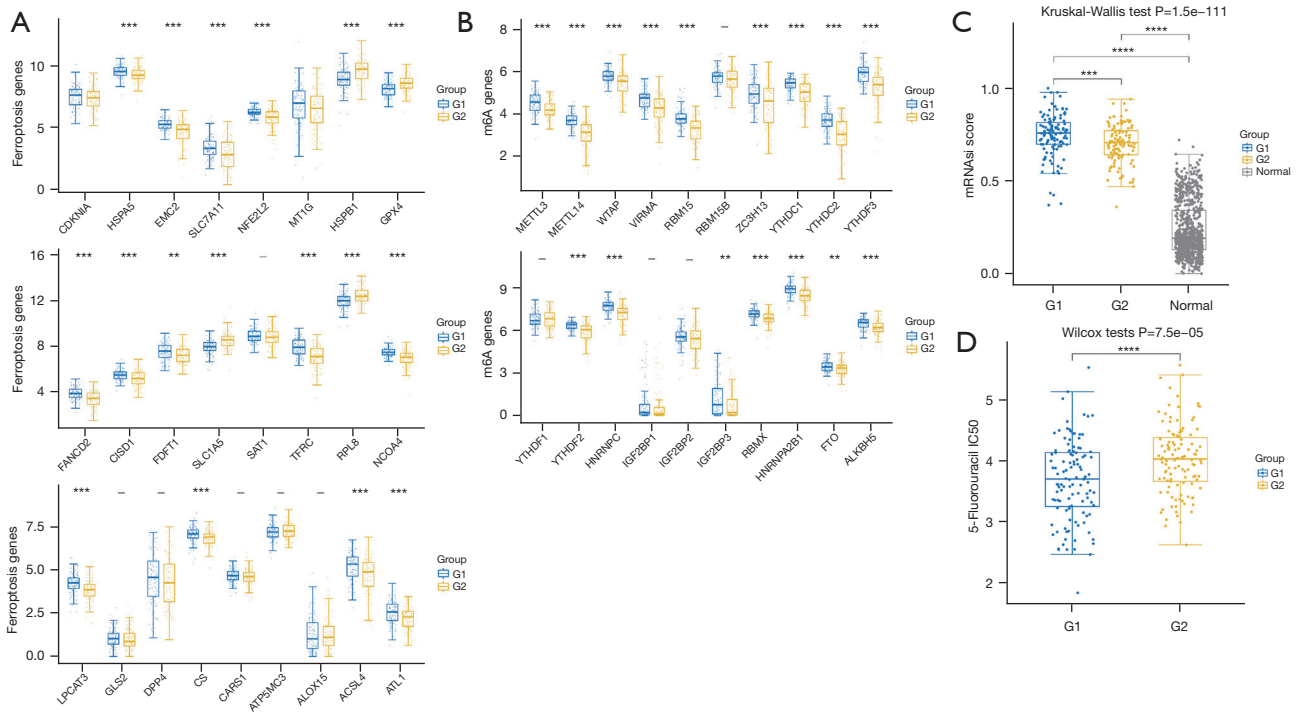

Figure 8 Analysis of functional mechanism related to *RPS6KA5*. (A) Box diagram showing the expression differences in the *RPS6KA5*$^{high25\%}$ and *RPS6KA5*$^{low25\%}$ group of FRGs. (B) m^{6}A methylation regulatory enzyme-related genes. (C) mRNAsi dryness index. (D) 5-FU IC50 values. G1: *RPS6KA5*$^{high25\%}$ group; G2: *RPS6KA5*$^{low25\%}$ group. –, not significant; **, P<0.01; ***, P<0.001; ****, P<0.0001. *RPS6KA5*, ribosomal protein S6 kinase A5; FRGs, ferroptosis-related genes; m6A, N6-methyladenosine; mRNAsi, messenger RNA stemness index; 5-FU, 5-fluorouracil; IC50, half-maximal inhibitory concentration.

and the IC50 value distributions of the *RPS6KA5*$^{high25\%}$ and *RPS6KA5*$^{low25\%}$ groups were compared. We found that the *RPS6KA5*$^{low25\%}$ group had significantly higher IC50 values that the *RPS6KA5*$^{high25\%}$ group (*Figure 8D*). This result indicated that the *RPS6KA5*$^{low25\%}$ group responded more poorly to 5-FU treatment.

Immune infiltration analysis

Based on the TIMER database, 'Gene' module analysis suggested that *RPS6KA5* expression was negatively correlated with tumor purity. After purity correction, *RPS6KA5* expression was found to be positively correlated with the infiltration abundance of B cells, CD8$^+$ T cells, CD4$^+$ T cells, macrophages, neutrophils, and dendritic cells in COAD (*Figure 9A*). 'sCNA' module analysis showed the difference in the immune cell infiltration ESTIMATE level among tumors with different CNA status of *RPS6KA5* in COAD. As shown in *Figure 9B*, the arm-level deletion of *RPS6KA5* was largely responsible for the infiltration levels of various immune cells types. The stromal, immune, and ESTIMATE scores of tumor samples were calculated. Correlation analysis showed that all three were positively correlated with the expression levels of *RPS6KA5* (*Figure 9C*), suggesting that the higher proportion of non-tumor cells increased with the expression level of *RPS6KA5*. This effect lowered tumor purity in COAD tissues.

Relationship between immunotherapy and RPS6KA5 expression

Immune checkpoint inhibitor (ICI) therapy has emerged as an important therapeutic method for patients with colon cancer. Currently, programmed cell death protein 1/programmed death ligand 1 (PD-1/PD-L1) expression status, tumor mutational burden (TMB), and microsatellite instability (MSI) as effective predictive markers for ICI treatment have been extensively studied. We investigated whether *RPS6KA5* expression affected the efficacy of immunotherapy in patients with COAD from multiple

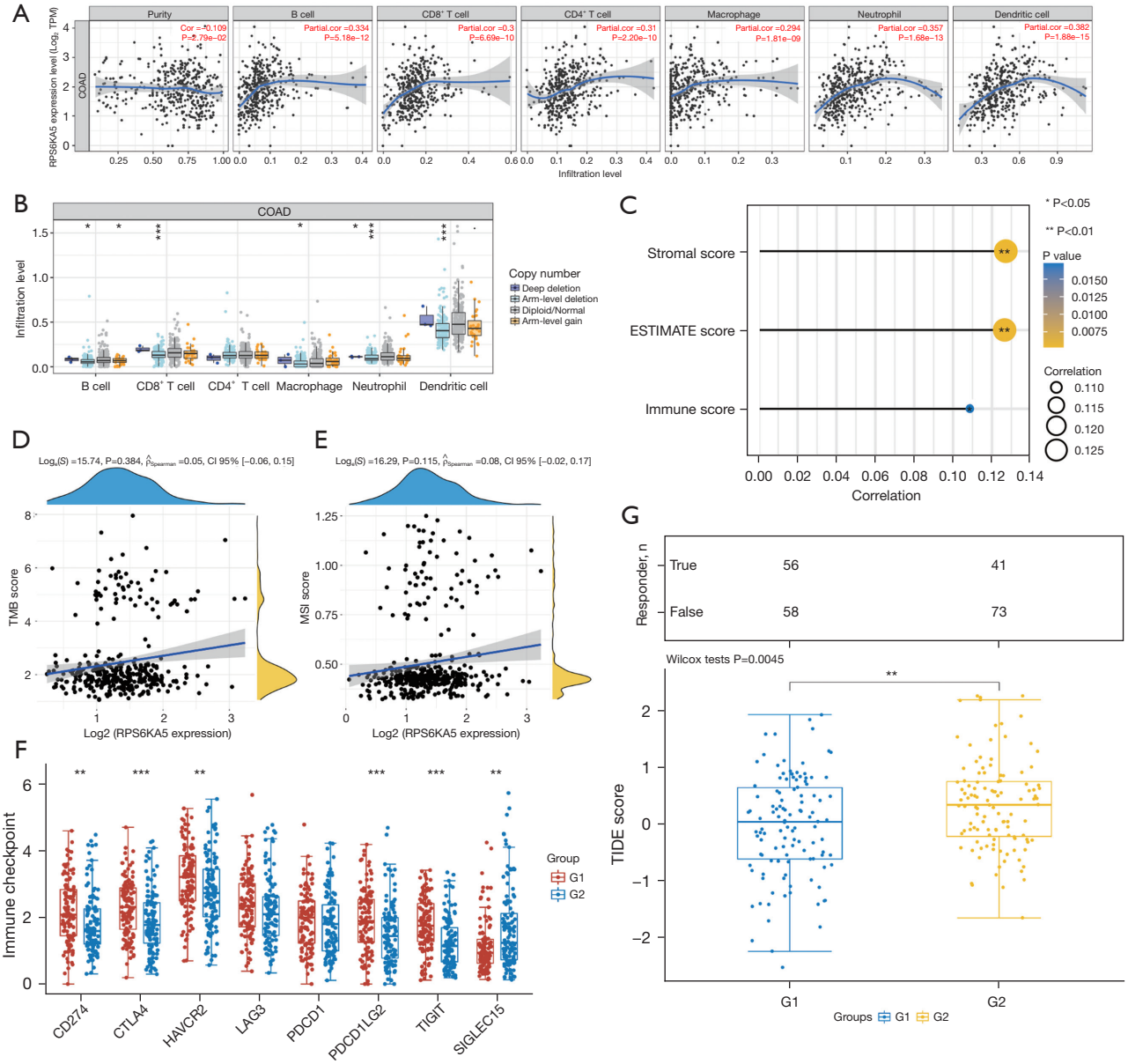

Figure 9 Analysis of immune infiltration and prediction of immunotherapy efficacy. (A) *RPS6KA5* expression was positively correlated with infiltration abundance of several immune cells. (B) Relationship between *RPS6KA5* copy number and tumor immune infiltration abundance. (C) Evaluation of colon-cancer immune infiltration based on the ESTIMATE algorithm: the stromal score, immune score, and comprehensive score were positively correlated with *RPS6KA5* expression. (D) No correlation existed between *RPS6KA5* expression and TMB. (E) No correlation existed between *RPS6KA5* expression and MSI. (F) Expression comparison of eight immune-checkpoint molecules in the RPS6KA5 high- and low-expression groups. (G) TIDE score between high- and low-expression groups of *RPS6KA5* (above: statistical table of immune responses of samples in the two groups; below: TIDE score distribution of samples in the two groups). G1: *RPS6KA5*$^{high25\%}$ group; G2: *RPS6KA5*$^{low25\%}$ group. *, P<0.05; **, P<0.01; ***, P<0.001. *RPS6KA5*, ribosomal protein S6 kinase A5; TPM, transcripts per million; COAD, colorectal adenocarcinoma; TMB, tumor mutational burden; CI, confidence interval; MSI, microsatellite instability; n, number; TIDE, tumor immune dysfunction and exclusion.

aspects. First, our analysis revealed that *RPS6KA5* expression had no correlation with TMB (*Figure 9D*) and MSI (*Figure 9E*). Second, given that the mechanism of immune checkpoint molecules expressed on immune cells facilitate tumor cell immune escape by inhibiting the function of immune cells (32), we performed corresponding analysis. The study revealed that the expression levels of the immune checkpoint molecules of *CD274* (PD-L1), *CTLA4*, *HAVCR2* (Tim-3), *PDCD1LG2* (PD-L2), and *TIGIT* were significantly increased in the *RPS6KA5*$^{high25\%}$ group, whereas *SIGLEC15* expression in *RPS6KA5*$^{low25\%}$ had a higher increase rate and the expression levels of *LAG3* (*CD223*) and *PDCD1* (PD-1) had no difference between the two groups (*Figure 9F*). Finally, the tumor immune dysfunction and exclusion (TIDE) calculation method (33) was used in assessing the likelihood of tumor immune escape and predicting response to ICI treatment. Compared with the *RPS6KA5*$^{low25\%}$ group, the *RPS6KA5*$^{high25\%}$ group had significantly higher TIDE scores (P=0.0045; *Figure 9G*), indicating that the *RPS6KA5*$^{high25\%}$ group had a higher possibility of immune escape and a poorer response to ICI treatment.

Discussion

CEACAM5 encodes CEA, a clinical biomarker for CRC, and contributes to tumorigenesis as a cell adhesion molecule (5,6). Our research identified a significant elevation in CEACAM5 expression within CRC tissues, which was found to be correlated with the prognostic outcomes of CRC. Increasing experimental evidence supports that the ceRNA regulatory network plays a role in diverse cancer types (34,35). However, the specific mechanisms and complex networks of the ceRNA regulatory pattern in COAD remain unclear. Given the pivotal role of CEACAM5 in COAD, we proceeded to construct the lncRNA-miRNA-mRNA triple networks correlated with CEACAM5 and establish a novel regulatory axis associated with prognosis in patients with COAD. Then, we explored the mechanisms and functions of this regulatory axis from a multi-omics perspective and attempted to corroborate the ceRNA regulatory pattern of lncRNA involvement in COAD.

We set up a ceRNA network of 18 lncRNAs, 177 miRNAs, and 25 mRNAs associated with CEACAM5 was constructed. *LCMT1-AS2* is located primarily in the cytoplasm, thereby meeting the prerequisites for lncRNA-miRNA interactions. In the prediction results, the ceRNA network regulated by *LCMT1-AS2* was largest and most complex. *LCMT1-AS2* was significantly positively correlated with *RPS6KA5*, and the key *LCMT1-AS2/miR-454-3p/RPS6KA5* regulatory axis was finally established after further correlation analysis of clinicopathological factors and survival analysis. In accordance with the ceRNA hypothesis, we speculated that *LCMT1-AS2* may competitively bind miR-454-3p to miRNA response elements, thereby affecting *RPS6KA5* expression. In our study, the functions and mechanisms of *RPS6KA5* were analyzed using the bioinformatic method, which indirectly reflected the mechanism of action of the regulatory axis of *LCMT1-AS2/RPS6KA5*.

By searching these three genes in PubMed, we found that the roles of miR-454-3p and *RPS6KA5* in cancer have been studied, whereas the mechanism of action of *LCMT1-AS2* is unknown and has not been explored by relevant research. MiR-454-3p can play a role as an oncogene in cervical cancer, glioma, stomach cancer, pancreatic cancer, malignant melanoma, and other solid tumors (36-40). Existing research *RPS6KA5*, also known as *MSK1*, *MSPK1*, or *RLPK*, plays a role in CRC. Bile acid upregulates *MUC2* transcription and contributes to carcinogenesis within colorectal tissues by activating the *EGFR/PKC/Ras/Raf-1/MEK1/ERK/CREB*, *PI3/Akt/IkappaB/NF-kappaB*, and *p38/MSK1/CREB* pathways (41). Vitamin D receptor acts as a transcription factor and a nongenomic activator of *p38MAPK-MSK1* and *RhoA-ROCK*, assisting $1,25(OH)_2D_3$ in inhibiting proliferation and promoting the differentiation of colon cancer cells (42). Our study found that *RPS6KA5* expression was downregulated in COAD tissues. Its copy number was significantly positively correlated with gene expression level, and low expression predicted poor OS. The abnormal expression of *RPS6KA5* may play a role in colon cancer through the PI3K-Akt signaling pathway. Additionally, we found that most FRGs were highly expressed in the *RPS6KA5*$^{high25\%}$ group, and this result indicated that the downregulation of *RPS6KA5* affects ferroptosis and inhibits the progression of colon cancer. This result is in line with the observations presented by Xie *et al.* that ferroptosis suppresses the growth of colon cancer (43). Several studies have shown that the abnormal methylation levels of m^6A are associated with stem cell differentiation (44), immune response (45), immune cell infiltration (46), tumorigenesis, and tumor cell proliferation and metastasis (47,48). The present study demonstrated that a significant decrease in *RPS6KA5* expression may lead to a decrease in the m^6A methylation modification and demodification/modification levels. It has been proven

that the increased expression of *YTHDF2*, *RBMX*, and *RBM15* was correlated with the activation of the *PI3K/Akt/mTOR* signaling pathways (49). Combined with the results of our KEGG enrichment analysis, the relationship between *RPS6KA5* expression dysregulation and the *PI3K-Akt* signaling pathway was further confirmed. Moreover, the mRNAsi index of colon cancer tissues was significantly increased compared with that of normal colon tissues and was higher in the *RPS6KA5*$^{high25\%}$ group than that in the *RPS6KA5*$^{low25\%}$ group. The *RPS6KA5*$^{low25\%}$ group responded more poorly to 5-FU therapy possibly because of enhanced resistance to 5-FU caused by significantly decreased *RPS6KA5* expression.

RPS6KA5 may affect the immune infiltration of COAD. The downregulation of *RPS6KA5* expression was accompanied by a significant decline in the infiltrating abundance of B cells, $CD8^+$ T cells, $CD4^+$ T cells, macrophages, neutrophils, and dendritic cells, decrease in the proportion of non-tumor cells, and increase in tumor purity in the colon cancer tissues. *RPS6KA5* expression was not correlated with TMB and MSI. However, correlation analysis on immune checkpoint molecules and TIDE algorithm showed similar results. That is, the *RPS6KA5*$^{high25\%}$ group had a higher likelihood of immune evasion and benefit less from ICI treatment.

PD-L1 and PD-1 expression levels weakly predict the responses of CRC patients to ICI treatment and are not commonly used as clinical predictors; meanwhile, patients with high microsatellite instability (MSI-H)/deficient mismatch repair (dMMR) CRC are sensitive to ICI treatment (50). In summary, significantly decreased *RPS6KA5* expression leads to decreased immune-cell infiltration abundance and weakened immune evasion. However, whether this change affects colon cancer progression and response to ICI treatment requires further study.

Conclusions

An *LCMT1-AS2/miR-454-3p/RPS6KA5* axis associated with COAD prognosis was established, which may be an important prognostic factor predicting the clinical outcome of COAD and may contribute to our understanding of lncRNA-miRNA-mRNA interactions. There are several limitations of this study that are worth discussing. First, our study is based on bioinformatics analysis, so the binding affinity of lncRNA-miRNA and miRNA-mRNA pairs obtained from the database should be verified experimentally. Second, more experimental studies on the mechanisms and functions of the *LCMT1-AS2/miR-454-3p/RPS6KA5* axis in COAD are imperative. Generally, our findings suggest that the *LCMT1-AS2/RPS6KA5* axis is a promising new candidate for potential prognostic biomarker and therapeutic target for COAD, which can be applied to facilitate individualized treatment strategies.

Acknowledgments

We sincerely acknowledge all the online databases for the availability of the data.
Funding: None.

Footnote

Reporting Checklist: The authors have completed the TRIPOD reporting checklist. Available at https://jgo.amegroups.com/article/view/10.21037/jgo-24-43/rc

Peer Review File: Available at https://jgo.amegroups.com/article/view/10.21037/jgo-24-43/prf

Conflicts of Interest: All authors have completed the ICMJE uniform disclosure form (available at https://jgo.amegroups.com/article/view/10.21037/jgo-24-43/coif). The authors have no conflicts of interest to declare.

Ethical Statement: The authors are accountable for all aspects of the work in ensuring that questions related to the accuracy or integrity of any part of the work are appropriately investigated and resolved. The study was conducted in accordance with the Declaration of Helsinki (as revised in 2013).

References

1. Sung H, Ferlay J, Siegel RL, et al. Global Cancer Statistics 2020: GLOBOCAN Estimates of Incidence and Mortality

Worldwide for 36 Cancers in 185 Countries. CA Cancer J Clin 2021;71:209-49.
2. Hao C, Zhang G, Zhang L. Serum CEA levels in 49 different types of cancer and noncancer diseases. Prog Mol Biol Transl Sci 2019;162:213-27.
3. Hatakeyama K, Wakabayashi-Nakao K, Ohshima K, et al. Novel protein isoforms of carcinoembryonic antigen are secreted from pancreatic, gastric and colorectal cancer cells. BMC Res Notes 2013;6:381.
4. Nicholson BD, Shinkins B, Pathiraja I, et al. Blood CEA levels for detecting recurrent colorectal cancer. Cochrane Database Syst Rev 2015;2015:CD011134.
5. Shinkins B, Nicholson BD, Primrose J, et al. The diagnostic accuracy of a single CEA blood test in detecting colorectal cancer recurrence: Results from the FACS trial. PLoS One 2017;12:e0171810.
6. Saeland E, Belo AI, Mongera S, et al. Differential glycosylation of MUC1 and CEACAM5 between normal mucosa and tumour tissue of colon cancer patients. Int J Cancer 2012;131:117-28.
7. van Gisbergen KP, Aarnoudse CA, Meijer GA, et al. Dendritic cells recognize tumor-specific glycosylation of carcinoembryonic antigen on colorectal cancer cells through dendritic cell-specific intercellular adhesion molecule-3-grabbing nonintegrin. Cancer Res 2005;65:5935-44.
8. Gu S, Zaidi S, Hassan MI, et al. Mutated CEACAMs Disrupt Transforming Growth Factor Beta Signaling and Alter the Intestinal Microbiome to Promote Colorectal Carcinogenesis. Gastroenterology 2020;158:238-52.
9. Kim T, Croce CM. Long noncoding RNAs: Undeciphered cellular codes encrypting keys of colorectal cancer pathogenesis. Cancer Lett 2018;417:89-95.
10. Salmena L, Poliseno L, Tay Y, et al. A ceRNA hypothesis: the Rosetta Stone of a hidden RNA language? Cell 2011;146:353-8.
11. Thomson DW, Dinger ME. Endogenous microRNA sponges: evidence and controversy. Nat Rev Genet 2016;17:272-83.
12. Wang P, Ning S, Zhang Y, et al. Identification of lncRNA-associated competing triplets reveals global patterns and prognostic markers for cancer. Nucleic Acids Res 2015;43:3478-89.
13. Poliseno L, Salmena L, Zhang J, et al. A coding-independent function of gene and pseudogene mRNAs regulates tumour biology. Nature 2010;465:1033-8.
14. Lin L, Zeng X, Liang S, et al. Construction of a co-expression network and prediction of metastasis markers in colorectal cancer patients with liver metastasis. J Gastrointest Oncol 2022;13:2426-38.
15. Mayakonda A, Lin DC, Assenov Y, et al. Maftools: efficient and comprehensive analysis of somatic variants in cancer. Genome Res 2018;28:1747-56.
16. Love MI, Huber W, Anders S. Moderated estimation of fold change and dispersion for RNA-seq data with DESeq2. Genome Biol 2014;15:550.
17. Sticht C, De La Torre C, Parveen A, et al. miRWalk: An online resource for prediction of microRNA binding sites. PLoS One 2018;13:e0206239.
18. Wang X. Improving microRNA target prediction by modeling with unambiguously identified microRNA-target pairs from CLIP-ligation studies. Bioinformatics 2016;32:1316-22.
19. Wong N, Wang X. miRDB: an online resource for microRNA target prediction and functional annotations. Nucleic Acids Res 2015;43:D146-52.
20. Chou CH, Shrestha S, Yang CD, et al. miRTarBase update 2018: a resource for experimentally validated microRNA-target interactions. Nucleic Acids Res 2018;46:D296-302.
21. Yu G, Wang LG, Han Y, et al. clusterProfiler: an R package for comparing biological themes among gene clusters. OMICS 2012;16:284-7.
22. Kang R, Kroemer G, Tang D. The tumor suppressor protein p53 and the ferroptosis network. Free Radic Biol Med 2019;133:162-8.
23. Liu Z, Zhao Q, Zuo ZX, et al. Systematic Analysis of the Aberrances and Functional Implications of Ferroptosis in Cancer. iScience 2020;23:101302.
24. Malta TM, Sokolov A, Gentles AJ, et al. Machine Learning Identifies Stemness Features Associated with Oncogenic Dedifferentiation. Cell 2018;173:338-354.e15.
25. Wang Z, Wang Y, Yang T, et al. Machine learning revealed stemness features and a novel stemness-based classification with appealing implications in discriminating the prognosis, immunotherapy and temozolomide responses of 906 glioblastoma patients. Brief Bioinform 2021;22:bbab032.
26. Yoshihara K, Shahmoradgoli M, Martínez E, et al. Inferring tumour purity and stromal and immune cell admixture from expression data. Nat Commun 2013;4:2612.
27. Laubert T, Bente V, Freitag-Wolf S, et al. Aneuploidy and elevated CEA indicate an increased risk for metachronous metastasis in colorectal cancer. Int J Colorectal Dis 2013;28:767-75.
28. Zhai H, Huang J, Yang C, et al. Serum CEA and CA19-

9 Levels are Associated with the Presence and Severity of Colorectal Neoplasia. Clin Lab 2018;64:351-6.
29. Liu J, Lichtenberg T, Hoadley KA, et al. An Integrated TCGA Pan-Cancer Clinical Data Resource to Drive High-Quality Survival Outcome Analytics. Cell 2018;173:400-416.e11.
30. Chen X, Kang R, Kroemer G, et al. Broadening horizons: the role of ferroptosis in cancer. Nat Rev Clin Oncol 2021;18:280-96.
31. Fu Y, Dominissini D, Rechavi G, et al. Gene expression regulation mediated through reversible m^{6}A RNA methylation. Nat Rev Genet 2014;15:293-306.
32. Topalian SL. Targeting Immune Checkpoints in Cancer Therapy. JAMA 2017;318:1647-8.
33. Hansen TB, Jensen TI, Clausen BH, et al. Natural RNA circles function as efficient microRNA sponges. Nature 2013;495:384-8.
34. Wu C, Hou X, Li S, et al. Identification of a potential competing endogenous RNA (ceRNA) network in gastric adenocarcinoma. J Gastrointest Oncol 2023;14:1019-36.
35. Zhang X, Han X, Zuo P, et al. CEACAM5 stimulates the progression of non-small-cell lung cancer by promoting cell proliferation and migration. J Int Med Res 2020;48:300060520959478.
36. Song Y, Guo Q, Gao S, et al. miR-454-3p promotes proliferation and induces apoptosis in human cervical cancer cells by targeting TRIM3. Biochem Biophys Res Commun 2019;516:872-9.
37. Zuo J, Yu H, Xie P, et al. miR-454-3p exerts tumor-suppressive functions by down-regulation of NFATc2 in glioblastoma. Gene 2019;710:233-9.
38. Jiang D, Li H, Xiang H, et al. Long Chain Non-Coding RNA (lncRNA) HOTAIR Knockdown Increases miR-454-3p to Suppress Gastric Cancer Growth by Targeting STAT3/Cyclin D1. Med Sci Monit 2019;25:1537-48.
39. Fan Y, Xu LL, Shi CY, et al. MicroRNA-454 regulates stromal cell derived factor-1 in the control of the growth of pancreatic ductal adenocarcinoma. Sci Rep 2016;6:22793.
40. Sun L, Wang Q, Gao X, et al. MicroRNA-454 functions as an oncogene by regulating PTEN in uveal melanoma. FEBS Lett 2015;589:2791-6.
41. Lee HY, Crawley S, Hokari R, et al. Bile acid regulates MUC2 transcription in colon cancer cells via positive EGFR/PKC/Ras/ERK/CREB, PI3K/Akt/IkappaB/NF-kappaB and p38/MSK1/CREB pathways and negative JNK/c-Jun/AP-1 pathway. Int J Oncol 2010;36:941-53.
42. Ordóñez-Morán P, Larriba MJ, Pálmer HG, et al. RhoA-ROCK and p38MAPK-MSK1 mediate vitamin D effects on gene expression, phenotype, and Wnt pathway in colon cancer cells. J Cell Biol 2008;183:697-710.
43. Xie Y, Zhu S, Song X, et al. The Tumor Suppressor p53 Limits Ferroptosis by Blocking DPP4 Activity. Cell Rep 2017;20:1692-704.
44. Wang S, Sun C, Li J, et al. Roles of RNA methylation by means of N(6)-methyladenosine (m(6)A) in human cancers. Cancer Lett 2017;408:112-20.
45. Han D, Liu J, Chen C, et al. Anti-tumour immunity controlled through mRNA m(6)A methylation and YTHDF1 in dendritic cells. Nature 2019;566:270-4.
46. Han S, Qi J, Fang K, et al. Characterization of m6A regulator-mediated methylation modification patterns and tumor microenvironment infiltration in acute myeloid leukemia. Cancer Med 2022;11:1413-26.
47. Cui Q, Shi H, Ye P, et al. m(6)A RNA Methylation Regulates the Self-Renewal and Tumorigenesis of Glioblastoma Stem Cells. Cell Rep 2017;18:2622-34.
48. Chen M, Wei L, Law CT, et al. RNA N6-methyladenosine methyltransferase-like 3 promotes liver cancer progression through YTHDF2-dependent posttranscriptional silencing of SOCS2. Hepatology 2018;67:2254-70.
49. Li Y, Xiao J, Bai J, et al. Molecular characterization and clinical relevance of m(6)A regulators across 33 cancer types. Mol Cancer 2019;18:137.
50. Oliveira AF, Bretes L, Furtado I. Review of PD-1/PD-L1 Inhibitors in Metastatic dMMR/MSI-H Colorectal Cancer. Front Oncol 2019;9:396.

Cite this article as: Liang F, Xu Y, Zheng H, Tang W. Establishing a carcinoembryonic antigen-associated competitive endogenous RNA network and forecasting an important regulatory axis in colon adenocarcinoma patients. J Gastrointest Oncol 2024;15(1):220-236. doi: 10.21037/jgo-24-43

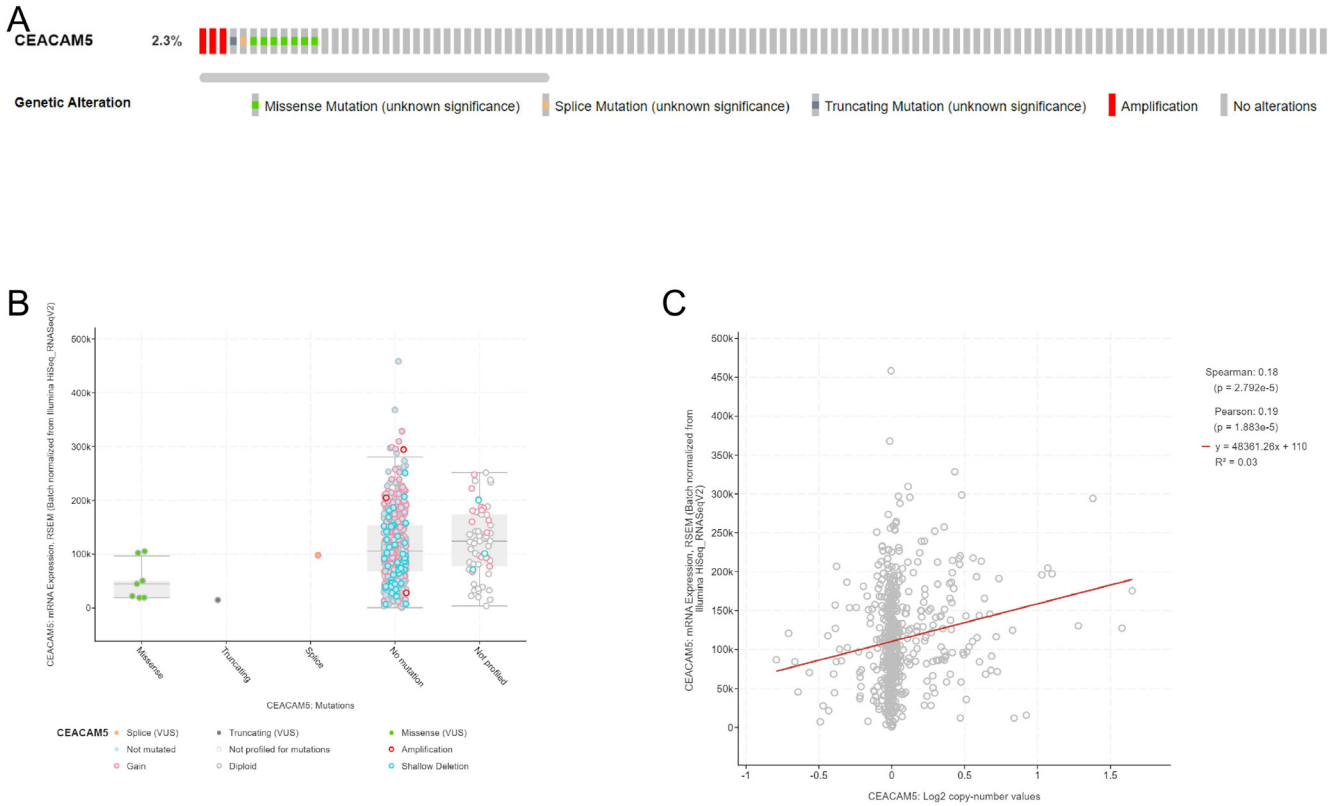

Figure S1 The genetic mutations and copy numbers of CEACAM5 in the TCGA-COAD dataset. (A) CEACAM5 genomic alteration of TCGA-COAD in the cBioPortal database. (B) Relationship between CEACAM5 genomic alteration and mRNA expression. (C) Relationship between CEACAM5 copy number and mRNA expression. RSEM, RNA-Seq by Expectation-Maximization; VUS, variant of uncertain significance; TCGA-COAD, The Cancer Genome Atlas colorectal adenocarcinoma; mRNA, messenger RNA.

https://dx.doi.org/10.21037/jgo-24-43

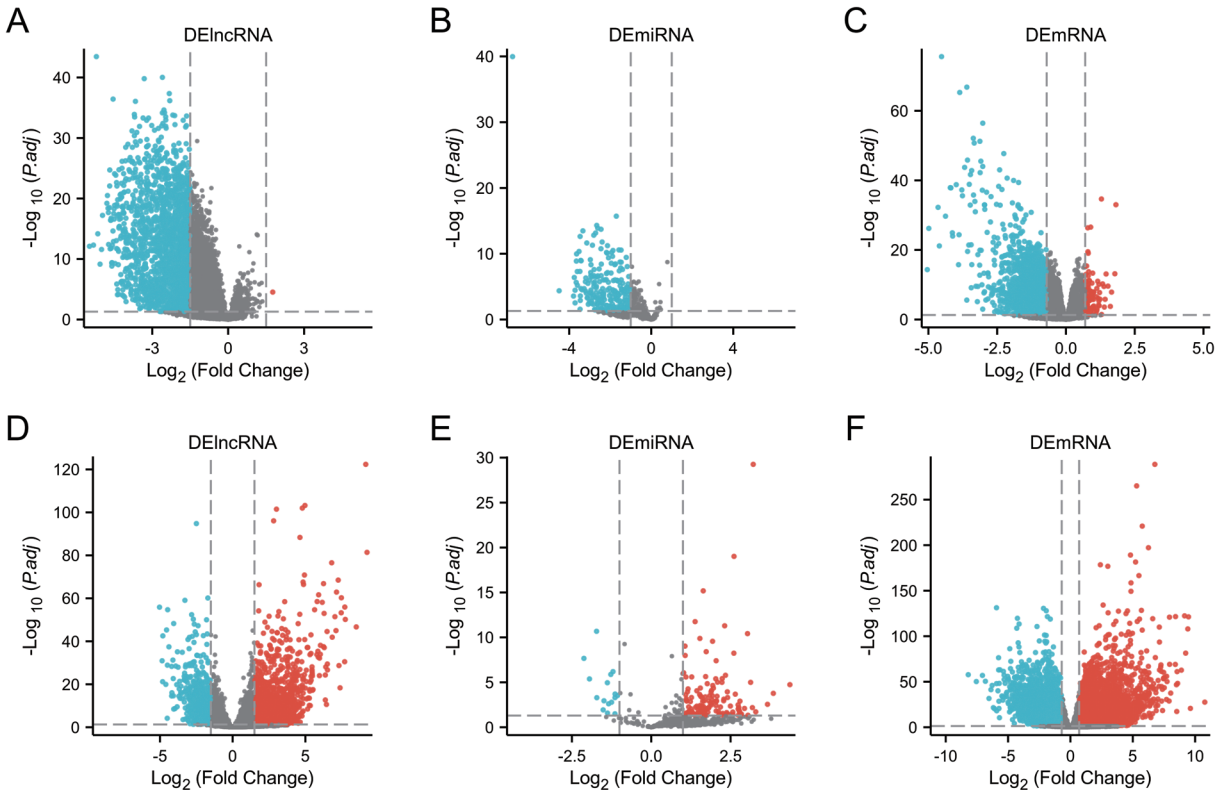

Figure S2 Volcano plots of differential analysis. (A-C) Volcano plots of differential genes between the high- and low-expression groups of CEACAM5. (D-F) Volcano plots of differential genes between colon cancer and paracancerous tissues (red represents upregulated genes, blue represents downregulated genes, and grey represents non-significant genes). P.adj, adjusted P value; DE, differentially expressed; lncRNA, long non-coding RNAs; miRNA, microRNA; mRNA, messenger RNA.

https://dx.doi.org/10.21037/jgo-24-43

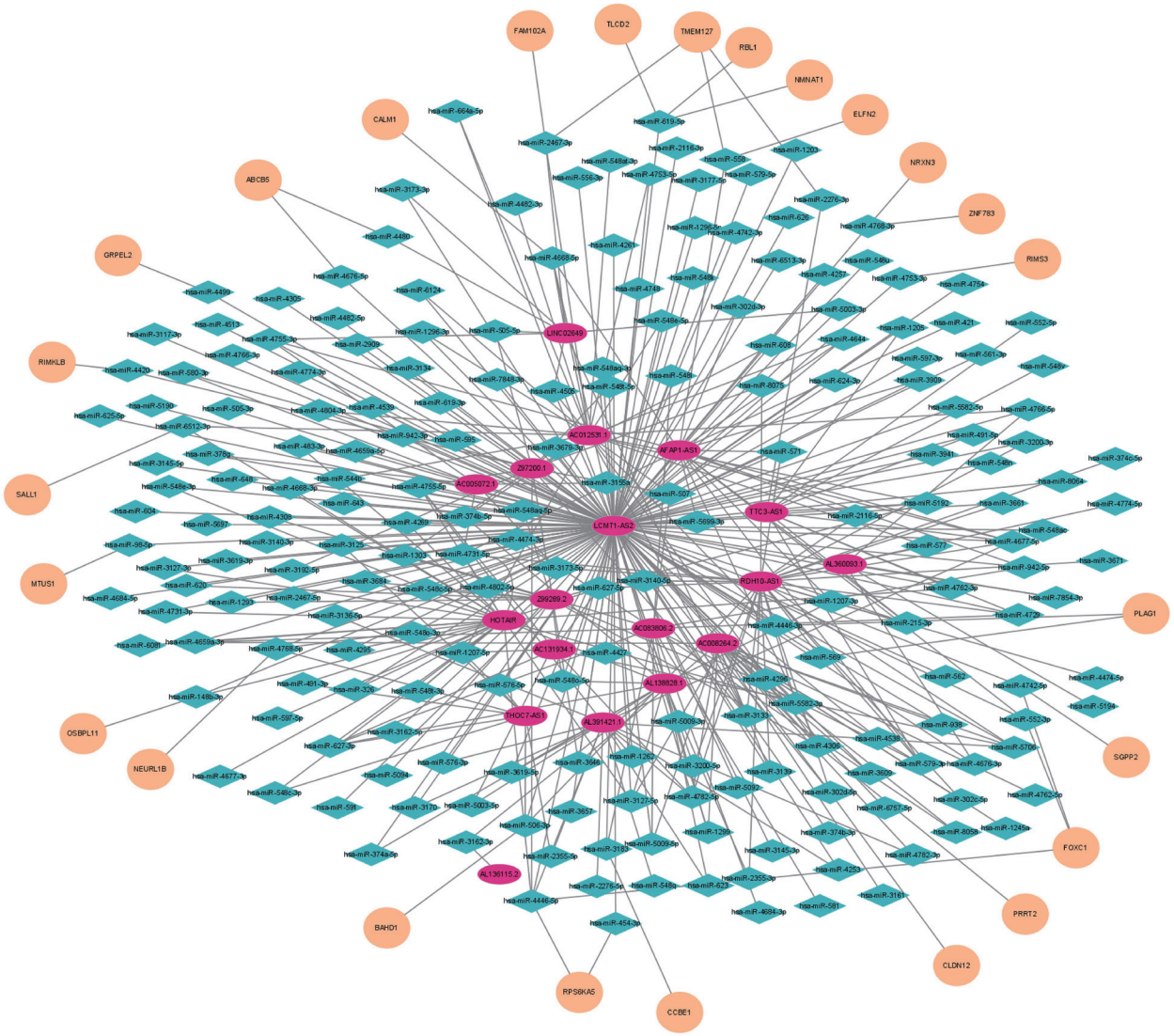

Figure S3 ceRNA networks diagram of 18 lncRNA-177 miRNAs-25 mRNAs. ceRNA, competitive endogenous RNA; lncRNA, long non-coding RNA; miRNA, microRNA; mRNA, messenger RNA.

https://dx.doi.org/10.21037/jgo-24-43

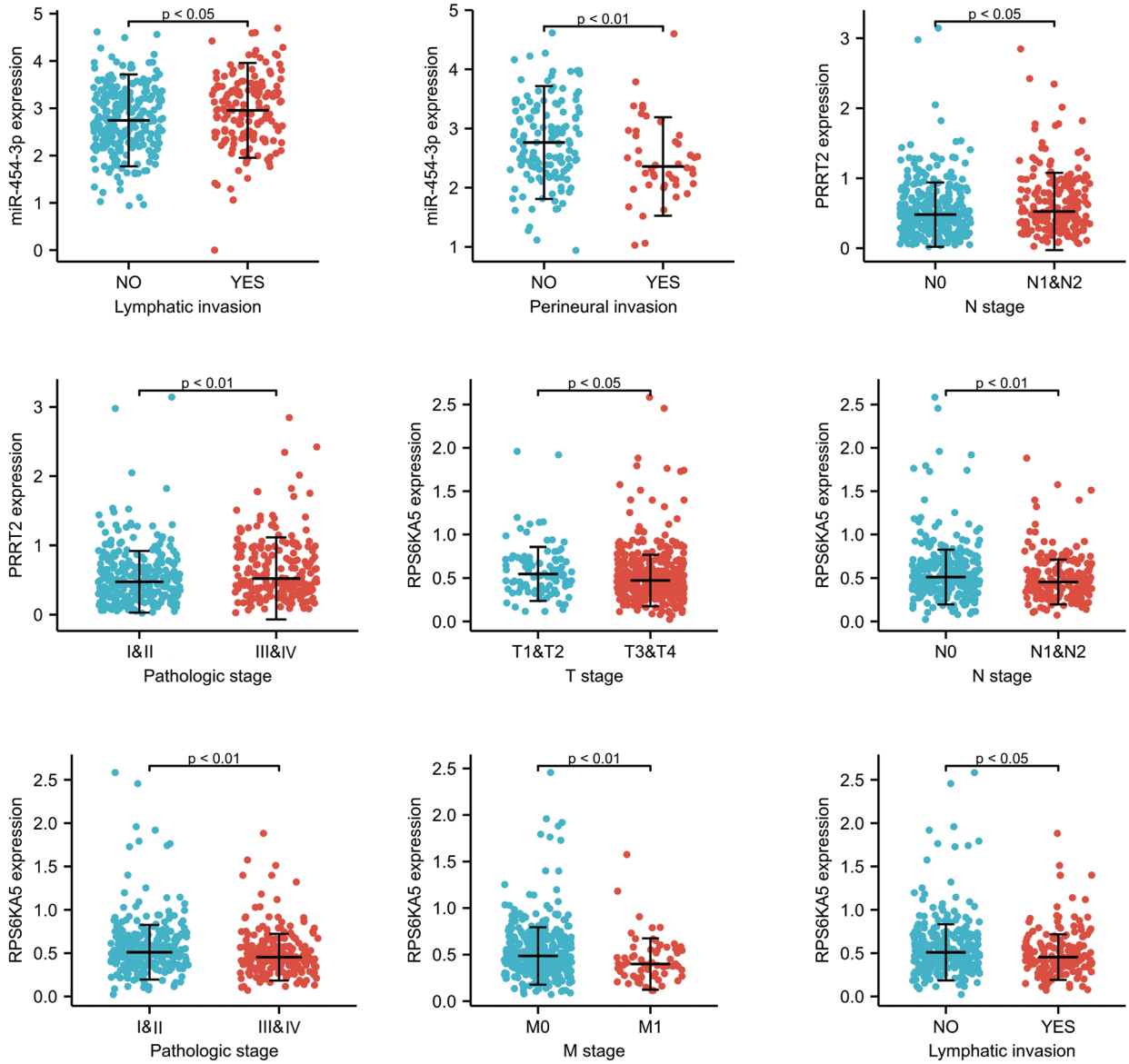

Figure S4 Correlation analysis between gene expression levels and clinical pathological factors.

https://dx.doi.org/10.21037/jgo-24-43

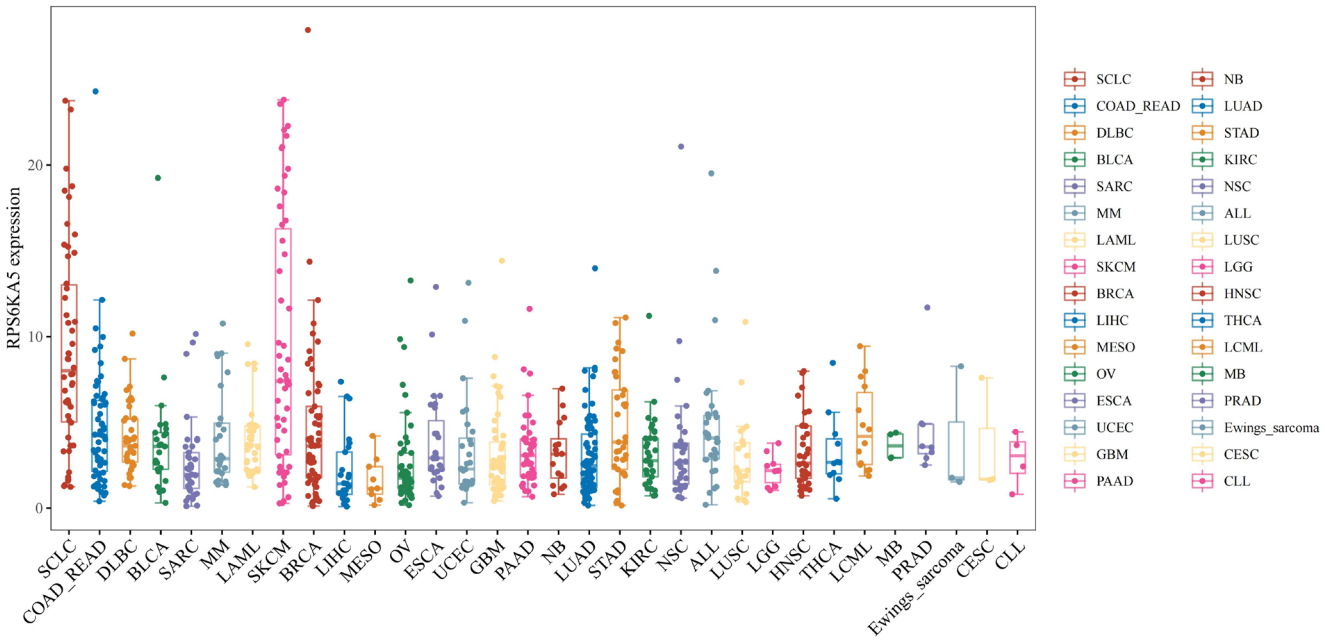

Figure S5 The *RPS6KA5* expression level of different cancer cell lines in the CCLE database (the x-axis represents different sample groups; the y-axis represents the distribution of gene expression). *RPS6KA5*, ribosomal protein S6 kinase A5; CCLE, Cancer Cell Line Encyclopedia.

https://dx.doi.org/10.21037/jgo-24-43

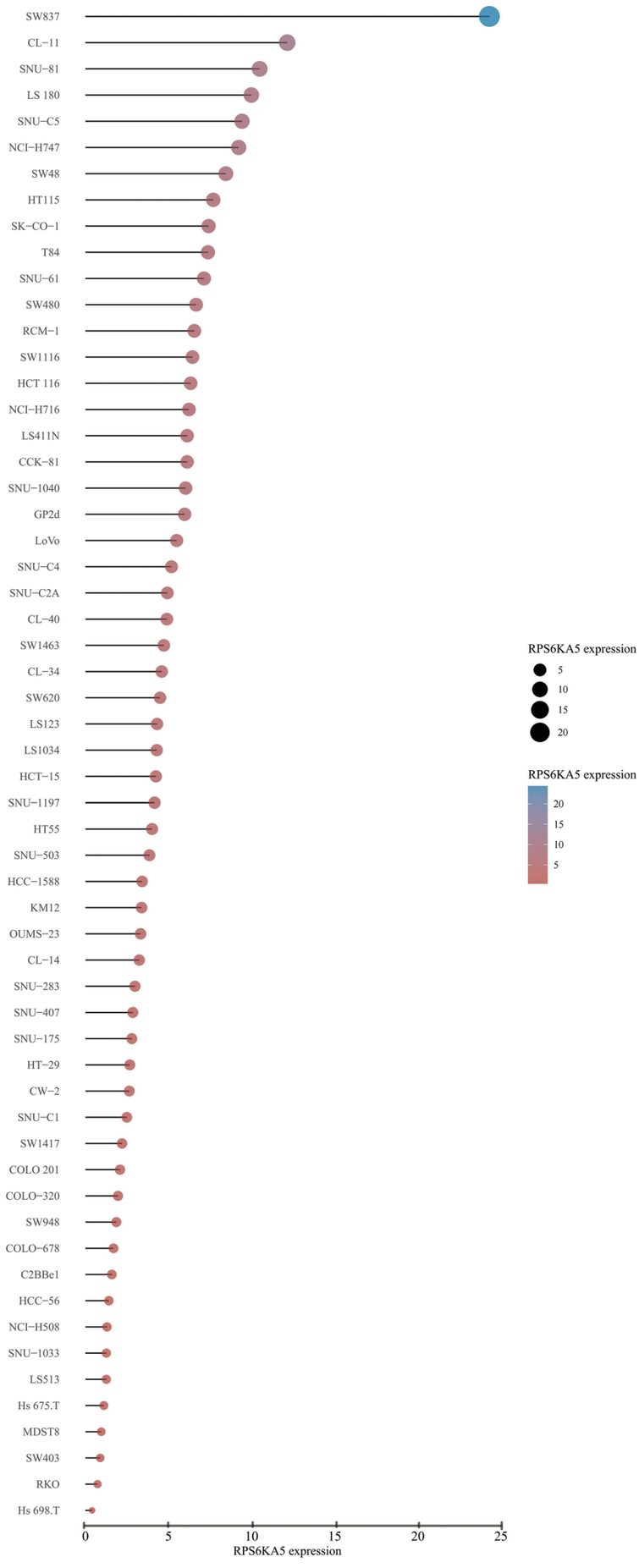

Figure S6 The distribution of *RPS6KA5* expression in different colorectal cancer cell lines in the CCLE database (the x-axis represents the status of gene expression, the y-axis represents different cell lines, the size of the dots in the figure indicates the level of expression, and different colors also signify the level of expression). *RPS6KA5*, ribosomal protein S6 kinase A5; CCLE, Cancer Cell Line Encyclopedia.

https://dx.doi.org/10.21037/jgo-24-43